Chitosan-based nanomaterials for drug delivery and antibiotic-free bacterial control

Vila-Sanjurjo C.* **, Fuenzalida J.P.*, Menchicchi B.*, Engwer C.*,
Hoffman S.*, Pereira S.*, Remuñán-López C.**, Alonso M.J.**, Vidal A.**, Moerschbacher B.M.*,
Kollenbrock S.*, Fetzner S.*, Philipp B.* and Goycoolea F.M.*

*Westfälische Wilhelms-Universität Münster - Schlossgarten 3, 48149 - Münster, Germany. Phone +49-2518324864, Fax +49-2518323823 goycoole@uni-muenster.de
**Department of Pharmacy and Pharmaceutical Technology. Univ. Santiago de Compostela, 15782 Spain

ABSTRACT

Research focused on chitosan (CS)-based nanostructured materials have become well-contrasted effective drug and gene delivery platforms, particularly for transmucosal administration. The biological properties of CS along with its capacity to harness stable colloidal particles able to associate and release drugs are key in the effectiveness of these systems *in vivo*. Chitosan characteristics (Mw and degree of acetylation), as well as the processing conditions to obtain nanoparticles, do influence the physical characteristics, stability in biological media and cytotoxic properties of nanoparticles and nanocapsules. A new type of hybrid particles obtained by physical and covalent co-crosslinking strategies exhibit a core-shell architecture with a shell of thickness 9.5-11.2 +/- 0.35 Aas evidenced by synchrotron SAXS (Figure 1). This platform is sought for the engineering of mucoadhesive nanomaterials for drug delivery and as a novel approach to achieve non-antibiotic antibacterial biodegradable materials.

Keywords: biopolymer, nanoparticles, chitosan, insulin, SAXS

INTRODUCTION

Research focused on chitosan-based nanostructured materials has burgeoned in the past decade or so, particularly in the biosciences and biotechnology (i.e. nanobiotechnology) fields. For instance, a recent search in the Web of Knowledge® since 1992 to date resulted in totally aprox. >~13,000 publications in chitosan-based nanomaterials, out of which, ~6,800 are directly in biology-related subject areas. The number of publications per year describes a steep rampant trend over the last decade, thus reflecting the high momentum of the research activity and intellectual property in this field.

Chitosan-based nanoparticles (NPs) harnessed by ionotropic gelation in absence of covalent crosslinking agents, as well as chitosan-based nanocapsules (NCs), were advanced in 1997 by the group of Prof. M.J. Alonso [1,2]. This type of chitosan-based nanoparticles are a well-established drug-delivey platform, particularly for the transmucosal delivery of biological macromolecules.

In turn, the use of covalent crosslinkers are able to confer CS greater stability against pH, temperature, biological and mechanical degradation [3]. Genipin (GNP) is a recently discovered natural crosslinking agent of chitosan that is sourced from the glycosilated geniposide that occur in the fruits of *Gardenia jasminoides* Ellis and Genipa americana. GNP has been reported to be much less cytotoxic and more compatible than other well-known chemical crosslinkers of CS, such as glutaraldehyde. Thus, the use of GNP as a crosslinker has become a promising alternative to develop fully biocompatible materials [4,5]. The chemical crosslinking reaction between GNP and CS takes place in two steps. The first and faster involves the nucleophilic attack on the GNP C3 carbon atom by a CS primary amine group and the formation of a GNP heterocyclic compound linked to a glucosamine residue. The second step is slower and consists in the nucleophilic substitution of the GNP ester group (C11), with the formation of a secondary amide linkage with CS and further formation of crosslinked bridges [4]. By controlling the extent of chemical crosslinking, other properties can be exploited, such as the ability of the resulting systems to adsorb and release biomolecules of particular interest for bionanotechnological or biopharmaceutical applications. This includes the capacity to target specific signals and receptors in bacteria, fungi and mammalian cells and to respond to physical and chemical stimuli.

A very active field of research is to develop alternative approaches to the indiscriminate use of antibiotics against pathogenic bacteria. In this respect, the development of new nanomaterials aimed to interfere with pathogenicity is of particular interest. *Quorum sensing* (QS) is a cell-cell communication mechanism involved in virulence and other behaviors, by which bacteria count their own numbers by producing and detecting the accumulation of signaling molecules [6]. The present paper addresses the recent advances in our understanding on the role of chitosan characteristics (Mw and degree of acetylation) on the physical characteristics and bioactive properties of chitosan-based nanomaterials. Proof-of-concept is presented here on the capacity of co-crosslinked CS-based

NPs to adsorb AHL molecules and hence, to potentially interfere with QS signaling in Gram (-) bacteria.

2 MATERIALS AND METHODS

2.1 Materials

CS was either a commercial sample of high purity grade in the hydrochloride salt form (ProtasanUP CL113, Mw ~125 kDa, DA ~14%, according to the manufacturer) purchased from Novamatrix (FMC-Biopolymer, Norway) or else a batch previously obtained from squid pen chitin kindly supplied by Dr. Dominique Gillet of Mahtani Chitosan Pvt Ltd (France). The characteristics for this CS sample were: Mw ~435 kDa, DA 1.6% (Ref No. 113 batch No 17/12/04) as described in previous studies. Genipin was purchased from Challenge Bioproducts (Taiwan). TPP and N-(3-oxo-hexanoyl)-L-homoserine lactone (3OC6HSL) were purchased from Sigma-Aldrich (Germany). Milli-Q water was used throughout. All reagents were of analytical grade.

2.2 Preparation of CS-TPP NPs

CS-TPP NPs were prepared according with the general ionotropic gelation protocol described by Calvo et al. [1] with minor modifications. In order to assess optimal composition to obtain NPs of average size <~200 nm and a low polydispersity (PDI ~0.1-0.2), different CS:TPP mass ratios were screened in two solvent environments, namely water or 85 mM NaCl. Briefly, 11.25 mL of the TPP solution were poured onto 18.75 mL of the CS solution under magnetic stirring (500 rpm). When necessary, NPs were isolated by centrifugation (40 min, 10000 x g, 25ºC) in 1.5 mL vials containing a glycerol bed and the pellets were resuspended in 100 µL of water.

2.3 Covalent co-crosslinking of CS-TPP NPs

The CS-TPP NPs were covalently co-crosslinked with GNP at different GNP:CS mass ratios (0.06:1 – 1.7:1). Aliquots of a GNP solution (5 mg/mL) were added to the NPs at a final concentration of 1 mg/mL in water. The NPs were incubated at 37ºC under shaking (~1400 rpm) for times ranging from 24-244 h.

2.4 Characterization of NPs

The size distribution of the nanoparticles was determined by dynamic light scattering using non-invasive back scattering (DLS-NIBS, measuring angle 173º) using a Malvern Zetasizer NanoZS ZEN 3600 (Malvern Instruments UK) equipped with a 4mW He/Ne laser beam operating at λ=633 nm. All measurements were performed at 25º ± 0.2 ºC. The kinetics of the crosslinking reaction were probed by UV/VIS spectroscopy (Beckman-Coulter DU® DU 730 - Life Science UV/Vis Spectrophotometer) and by synchrotron small-angle X-ray scattering (SAXS, ESRF Grenoble, France; BM02-D2AM, E = 14 kEv; sample-to-detector distance: 1.51 m).

2.5 Cytotoxic properties of chitosan-based nanoparticles

Two different human lymphoblastic-derived cell lines were utilized, namely K562 and THP1, which are able to grow in suspension (in complete RPMI medium) and hence require little manipulation. Equivalent doses of CS in all treatments were applied to cells (~1.0 x 104 cells/mL) during 24 or 48 h. Prior to FACS analysis (FACScalibur, BD Biosciences), the cells were washed and stained with propidium iodide (PI). The percentage of dead cells (i.e. PI positive), was detected in the red FL2 channel; while that of viable cells was calculated by difference.

2.6 Evaluation of the adsorption capacity of QS signals by CS-TPP NPs using a fluorescence *E.coli* biosensor

The BioBrick standard biological part BBa_T9002, ligated into the pSB1A3 (http://partsregistry.org/Part:BBa_T9002) was a gift sample from Prof. Anderson Lab (UC Berkeley, USA). The part BBa_T9002 was transformed by chemical transformation into *E. coli* Top 10 (Invitrogen, Life Technologies Co., UK) and stored in a 30% glycerol stock at -80ºC. The part BBa_T9002 comprises the transcription factor (LuxR), which is constitutively expressed but it is active only in the presence of a cell-cell signaling molecule (3OC6HSL), which acts as an exogenous input. At an adequate concentration, two molecules of 3OC6HSL bind to two molecules of LuxR and activate the expression of GFP (output), under the lux pR promoter from *Vibrio fischeri*. The fluorescence biosensor was calibrated for different 3OC6HSL concentrations as described in Canton et al [7]. Twenty µL aliquots of the different 3OC6HSL solutions were transferred into the wells of a flat-bottomed 96-well plate (Greiner Bio-One, cat. # M3061) and 180 µL aliquots of the bacterial culture were added to each well to yield AHL final concentrations ranging from 1E-12 to 1E-2 M). Blank wells were filled with 200 µL of medium to measure the absorbance background. Control wells were filled with 180 µL of bacterial culture and 20 µL of water to measure the fluorescence background. The plate was incubated in a Safire Tecan-F129013 Microplate Reader (Tecan, Crailsheim, Germany) at 37ºC and assayed with an automatically repeating protocol of fluorescence measurements (λex=485 nm and λem=520nm, 40 µs, 10 flashes, gain 100, top fluorescence), absorbance measurements (OD600) (λ=600 nm absorbance filter, 10

flashes) and shaking (5 s, orbital shaking, high speed). Time between repeated measurements was 6 min. For each experiment, the fluorescence intensity (FI) and OD600 data were corrected by subtracting the values of absorbance and fluorescence backgrounds and expressed as the average for each treatment. Data was represented in terms of FI/OD600 versus incubation time. For the calibration of the biosensor, the rate of the evolution of FI/OD600 was estimated from the value of the slope of a linear fit of FI/OD600 during the first 100 min of incubation. The dependence of rate of FI/OD600 as a function of AHL concentration was fitted to a non-linear growth sigmoidal Hill function by a minimization iteration process (OriginPro 8G, OriginLab Co., MA, USA) that allowed to determine the best-fit parameters. All measurements were conducted in triplicate.

To test the adsorption efficiency of the co-crosslinked CS NPs towards 3OC6HSL, 2.5E-09 M AHL was incubated in 1.5 mL vials with 1 mg/mL of non-isolated CS-TPP NPs (CS:TPP mass ratio 3.33:1), both in the presence and absence of GNP (final GNP:NP mass ratio 0.24:1), at 37ºC with shaking (100 rpm), for 24 h. As controls the same concentration of AHL was incubated both alone or in the presence of GNP, without NPs. The final volume was 1 mL in all cases and all the reaction vials were prepared in triplicate. The vials were centrifuged 13,000 rpm at room temperature for 30 min and 20 µL of the supernatants were applied to the fluorescence E.coli biosensor, to record the OD600 and FI, as previously described.

3 RESULTS AND DISCUSSION

Inspection of the Figure 1 reveals that the mass ratio of CS/TPP plays an important role on the final NP size and polydispersity (results not shown), showing that it is possible to obtain NPs with a size of ~200 nm and a fairly low PDI~0.2-0.3 under a narrow range of CS:TPP mass ratios ~3:1- 4:1 in 85 mM NaCl. Other studies have reported that the ionic strength affects the NP size, since the addition of monovalent ions to the solutions may overcome the electrostatic repulsion of the charged amino groups, leading to an increased flexibility and compaction of the CS backbone [10].

A new type of hybrid particles with pH sensitivity have also been obtained by covalent co-crosslinking and loaded with insulin (Figure 2). The insulin release behavior of these nanoparticle systems (results not shown) has revealed that the systems that are crosslinked with genipin are able to retain insulin in SGF (pH 1.2), while those which are not crosslinked, released the peptide almost immediately under these conditions. This behavior cannot be ascribed to a change in the nanoparticle shell thickness, as no differences were noticed between uncrosslinked and crosslinked nanoparticles. In simulated intestinal fluid (pH 6.8), the insulin loaded nanoparticles that were crosslinked exhibited a larger interfacial thickness than that attained in SGF and also than the non-crosslinked particles in SIF.

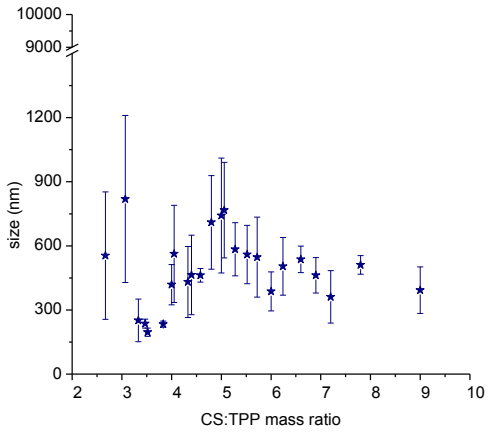

Fig. 1. Z-average size of chitosan-TPP nanoparticles at varying CS:TPP mass ratio (NaCl 85mM; 25°C).

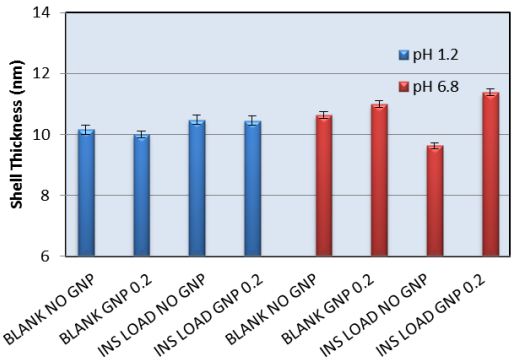

Fig. 2. Core-shell model fit of synchrotron SAXS scatter intensity data for insulin-loaded chitosan-TPP nanoparticles co-crosslinked with genipin (water; 25°C).

Yet another aspect evaluated was the effect of CS-TPP nanoparticles made of CS of varying DA and Mw on the cell viability relative to untreated cells. Lower cell viability was observed only for CS HDP DA 1% (Figure 3). Noticeably, a lower cytotoxicity was observed when the same CS was applied in the form of NPs or NCs. Moreover, while a dose-response effect was evident for both the chitosan solution and the NPs, it was practically inexistent for comparable doses of NCs. Essentially similar results were observed for both cell lines and for exposure times of 24 or 48 h in the two cell lines tested.

The results of this study agree well with previous evidences reported in the literature of an enhanced cytotoxic effect promoted by chitosans with low DA [11]. The lower cytotoxicity observed for CS NPs, and especially so for NCs, highlights their great potential as cellular nanocarriers for bioactive molecules (e.g. genetic material) with enormous potential relevance in nanomedicine.

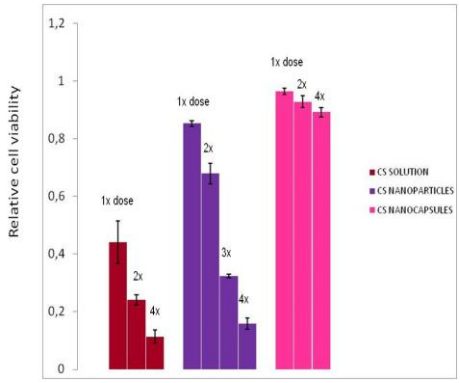

Fig. 3. Dose effect of different systems (CS solution, nanoparticles and nanocapsules) made of CS HDP DA 1% on the cell viability (K562 cell line) (1x CS dose = 67 µg/well, 24 h treatment).

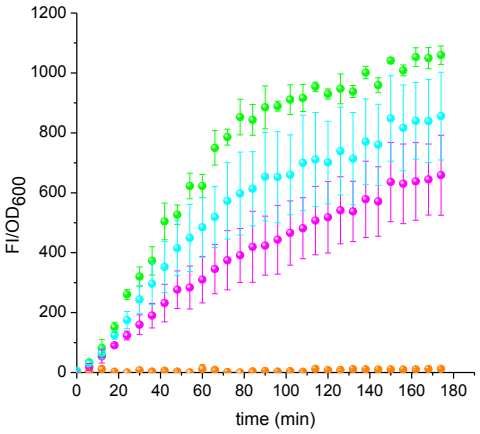

Fig. 4. Effect of the co-incubation of NPs with AHL on FI (A), bacterial OD600 (B) and normalized FI/OD600 (C), after 3h treatment of the E.coli biosensor with the supernatants. (D) Effect of the different treatments on the rate of FI/OD600 during the first 55 minutes of bacterial growth represented as mean ± standard deviation (n=3)

Figure 4 shows the effect of the co-incubation of NPs with AHL on FI (A), bacterial OD600 (B) and normalized FI/OD600 (C), after 3 h treatment of the E.coli biosensor with the supernatants. Figure 6D reveals the effect of the different treatments on the rate of FI/OD600 during the first 55 min of bacterial growth. As shown in the plots, the fluorescence response is reduced and retarded in the case of the NP treatments, being more acussed for the co-crosslinked NPs, when compared with the control AHL, which was not pre-incubated with NPs. The reduced fluorescence cannot be related to any toxic effect of the treatments as evidenced by the response of the optical density (OD600). Hydrophobic interactions seem to be at play in governing the enhanced AHL adsorption to co-crosslinked NPs, as previously reported for other CS-GNP hybrid materials aimed to the adsorption of poor soluble molecules [3].

ACKNOWLEDGEMENTS

Support from European Commission 7th Framework Marie Curie programme – BioNanoSmart_DDS–No. 221111; by the "Consolidation and estructuration of competitive research unitsde (Competitive Reference Groups)", REF. 2010/18, and by FEDER Financiation (Spain). C.V. acknowledges the pre-doctoral fellowships granted from Xunta de Galicia and Ministerio de Educación y Ciencia (FPU) and the Research Fellowships granted from the DAAD (Germany) and Fundación Pedro Barrié de la Maza. Projects No. SC2774 and CH 3386 of European Synchrotron Research Facility (Grenoble, France) and Project FIS PS09/00816 from the Spanish Government-ISCIII are also gratefully acknowledged. FMG, JPF, BM, BMM are grateful to DFG (Germany) for the IRTG Indo-German MCGS ("Molecular and Cellular Glyco-Sciences") programme.

REFERENCES

[1] Calvo et al. J. Appl. Polym. Sci. 63, 125–132. 1997
[2] Calvo et al. Colloid Polym. Sci. 275 (1997), 46–53. 1997
[3] Espinosa-García et al. Biomacromolecules, 8, 3355-3364. 2007
[4] Moura, M.J. et al. Biomacromolecules 12, 3275-3284. 2011
[5] Butler, M.F. et al. J. Polym. Sci. A Polym. Chem., 41, 3941-3953
[6] Bassler & Losick.. Cell, 125, 237-246. 2006
[7] Canton et al. Nat. Biotechnol., 26 (7), 787-793. 2008
[10] Jonassen et al. Colloid. Polym. Sci., 290, 919-929. 2012
[11] Huang M. et al. Pharm. Res., 2, 344. 2004